WATER RESOURCES RESEARCH, VOL. 37, NO. 3, PAGES 759–769, MARCH 2001

Isotopic evolution of a seasonal snowpack and its melt

Susan Taylor,[1,2] Xiahong Feng,[2] James W. Kirchner,[3] Randall Osterhuber,[4] Björn Klaue,[5] and Carl E. Renshaw[2]

Abstract. The study of isotopic variation in snowmelt from seasonal snowpacks is useful for understanding snowmelt processes and is important for accurate hydrograph separation of spring runoff. However, the complex and variable nature of processes within a snowpack has precluded a quantitative link between the isotopic composition of the original snow and its melt. This work studies the isotopic composition of new snow and its modification by snow metamorphism and melting. To distinguish individual snowstorms, we applied solutions of rare earth elements to the snow surface between storms. The snowmelt was isotopically less variable than the snowpack, which in turn was less variable than the new snow, reflecting isotopic redistribution during metamorphism and melting. The snowmelt had low $\delta^{18}O$ values early in the season and became progressively enriched in ^{18}O as the pack continued to melt. On a given day, meltwater $\delta^{18}O$ was systematically lower whenever melt rates were low than when melt rates were high. The progressive enrichment in $\delta^{18}O$ of snowmelt and the dependence of $\delta^{18}O$ on melt rates can be explained by isotopic exchange between liquid water and ice. A one-dimensional (1-D) model of the melting process, including advection and water-ice isotopic exchange kinetics, reproduces the observed progressive ^{18}O enrichment of snowmelt.

1. Introduction

In temperate regions, snowmelt can account for the majority of the water added to a catchment and often causes the largest annual stream discharge event [*Rodhe*, 1998]. The path taken by snowmelt to a stream has important implications for flood prediction, resource management, water budgets, and heat and chemical fluxes to rivers [e.g., *Prowse and Conly*, 1998; *Johannessen and Henriksen*, 1978]. One method to ascertain the contribution of snowmelt to spring discharge is through a hydrograph separation using oxygen or hydrogen isotopes of meltwater, stream water, and groundwater [*Dinçer et al*., 1970; *Sklash and Farvolden*, 1979]. In this approach, groundwater and snowmelt are considered to be preevent and event water, respectively. If these two water sources are isotopically different but homogeneous over the timescale of the hydrograph, the stream water can be "separated" into its two contributing components using mass balance calculations. In a number of applications [e.g., *Rodhe*, 1981; *Bottomley et al*., 1986] the isotopic value of the meltwater has been obtained from snow cores, and it has been assumed constant throughout the melt season.

However, both field [*Hooper and Shoemaker*, 1986] and laboratory [*Herrmann et al*., 1981] experiments show significant differences between the isotopic composition of meltwater and the "average" isotopic value of the snowpack used for hydrograph separation. *Hooper and Shoemaker* [1986] measured a 30‰ change in the δD values of meltwater collected at the base of the pack and a 60‰ change during rain-on-snow events. Laboratory experiments, where homogeneous snow columns were melted under diurnal conditions, showed up to 20‰ variability in δD in the meltwater [*Herrmann et al*., 1981]. These observed isotopic variations in meltwater need to be taken into account to obtain accurate hydrograph separations [*Genereux*, 1998; *Feng et al*., 1998] and to determine the mechanism(s) by which water is delivered to a stream [*Buttle*, 1994].

In this paper, we describe results of field and laboratory studies of the oxygen isotopic evolution of a snowpack and its melt. The objective of the research was to understand variables that affect the isotopic compositions of snowmelt throughout the season, from snow accumulation through snow melting. The field study was conducted during the winter of 1997–1998 at the Central Sierra Snow Laboratory (CSSL) in California. To monitor the isotopic change from new snow, through snow metamorphism, to snowmelt, we used rare earth element chlorides to distinguish the snow layers deposited by individual storms. We also conducted laboratory experiments in a cold room at the Cold Regions Research and Engineering Laboratory (CRREL). We melted snow under well-controlled conditions so that the physical parameters that affect the isotopic composition of the meltwater could be obtained using a physically based model.

2. Site Information and Experimental Methods

2.1. Field Site

The Central Sierra Snow Laboratory is located at 2100 m on the southwest crest of the Sierra Nevada near Soda Springs, California (39°22′19″N and 122°22′15″W). The site receives ~80% of its precipitation in the form of snow. Usually, snow begins to accumulate in November and continues through May. On average, the annual snowpack at CSSL has ~90 cm of

[1]U.S. Army Cold Regions Research and Engineering Laboratory, Hanover, New Hampshire.
[2]Department of Earth Sciences, Dartmouth College, Hanover, New Hampshire.
[3]Department of Earth and Planetary Science, University of California, Berkeley, California.
[4]Central Sierra Snow Laboratory, Soda Springs, California.
[5]Department of Geological Sciences, University of Michigan, Ann Arbor, Michigan.

Paper number 2000WR900341.
0043-1397/01/2000WR900341$09.00

water equivalent [*Osterhuber*, 1999]. Snowfall has been measured in this area since 1879, providing the longest record in the western United States. The 1997–1998 year was characterized by a large El Niño event, and the measured annual precipitation was the sixth largest on record [*Osterhuber*, 1999], with a snow water equivalent of ~200 cm.

The snow laboratory is in a 0.5-hectare clearing in a pine forest. It is instrumented to measure meteorological variables, including air temperature, precipitation, wind speed, humidity, and incident and reflected radiation. Two 6 × 3-m melt pans collect water draining from the overlying snowpack. The north melt pan (the one we used) slopes gently to a corner drain. The meltwater then flows underground along 8-m of PVC pipe to a hut where the flow rate is recorded using a 4-L tipping bucket attached to a data logger.

2.2. Field Experiments

2.2.1. Rare earth element tracers. To study the isotopic changes occurring in the pack and in the melt, we need to be able to distinguish individual snow layers. Others have used pieces of colored string or ribbon [*Judy et al*., 1970; *Martinec et al*., 1977]. We used chloride solutions of the rare earth elements. The rare earth elements (REEs) include lanthanum (^{57}La) and the lanthanide elements (atomic number of 58 to 71). The very low natural abundance (typically several parts per trillion) of the REEs allowed us to make tracer solutions with concentrations at least 6 orders of magnitude greater than their background concentrations in clean snow. The freezing point depression is calculated to be <1/500°C for a 50 ppm REE chloride solution. REEs can therefore serve as sensitive tracers at concentrations that do not significantly alter the snow's properties. To detect possible chemical processes that may differentiate the REE tracers, we used La as a common tracer in all REE solutions.

Each tracer solution contained about 25 ppm La and 25 ppm of one other REE and was prepared from ultrapure (99.99%) REE chlorides. After each large snowstorm, ~3 L of the tracer solution were sprayed onto the snow surface overlying the northern melt pan, using a compressed air sprayer fitted with a fine spray nozzle. A small aliquot of each spray solution was collected for an accurate determination of its concentration. When possible, we applied the tracers between storms in subzero temperatures to minimize leaching of the tracers by meltwater or rain.

To examine the position of the applied tracers in the snow profile, we sprayed another 6 × 3 m^2-area 4 m from the melt pan. Here we dug snow pits before the melting season. Eight tracers, including Ce, Pr, Nd, Sm, Eu, Gd, Tb, and Dy, were applied to both areas between December and April.

2.2.2. Sampling. Three types of samples were collected: new snow, snow pit layers, and snowmelt. New snow, from storms depositing more than 15 cm of snow, was collected using a Plexiglas sampling corer. For snowfalls >60 cm a sample was taken for each 60 cm. The density of each sample was measured; the sample was then melted in precleaned plastic bags and transferred into bottles washed with Citranox®. During the season we sampled 1010 out of 1345 cm of new snow, or ~75% of the total volume. The remaining 25% fell as small amounts throughout the season.

Before the onset of the spring melt we sampled four snow pits. Three were in the REE-sprayed area, and the fourth, used as a control, was in a separate area where no REE tracers were sprayed. The control pit and one REE pit (pit A) were sampled on March 23, 1998, and the other two (pits B and C) were sampled on April 9. The snowpack was ~3 m deep, and we sampled the entire profile at 10-cm increments. A stainless steel, 10-cm-wide, wedge-shaped snow sampler (1000 cm^3) was used to collect the snow and was weighed to obtain the snow density. The samples were then transferred into clean plastic bags. To avoid cross-contamination, the stainless steel sampler was rinsed with distilled water between samples. After melting at room temperature an aliquot of each sample was transferred into a 125-mL plastic bottle.

Meltwater samples were collected from the tipping bucket that measured flow from the north melt pan. The melt rate was slow early in the season, and we sampled infrequently. When the melt rate increased, we sampled twice daily, once in the morning and once in the afternoon. Approximately 60,000 L of melt were measured by the tipping bucket. The measured outflow was 50% higher than the value expected on the basis of the measured snow water equivalent (~200 cm), indicating that the water from an area outside the melt pan added to the measured outflow. Since we did not observe well-developed ice layers, we do not think much lateral flow occurred. Rather, the added water came from the surface with an area larger than the dimensions of the pan. The additional area would be ~9 m^2, equivalent to expanding the melt pan by 40 cm on each side. This increase is a small fraction of the melt pan dimensions (14% and 7% of the short and long sides of the pan, respectively), and we do not think the extra flow significantly deviates from 1-D flow, an assumption used later in this paper.

2.3. Cold Room Experiments

To help in interpreting our field data, we conducted two controlled experiments in a −1°C cold room at CRREL. Natural snow was sieved and mixed thoroughly, and three random samples were taken to test for isotopic homogeneity. We then sieved the snow into a Plexiglas column (90 cm high with a 12.5-cm inside diameter) resting upon a plastic screen and funnel. The snow was melted at the top using an infrared heat lamp suspended inside the Plexiglas column. The lamp was moved down frequently so that it remained ~50 cm from the snow surface and melted the snow at a constant rate. The Plexiglas column was wrapped in insulation, a small section of which could be removed to check the snow depth and to adjust the height of the lamp. From the funnel, meltwater flowed down a heated plastic tube to an automatic fraction sampler.

In the first experiment we measured the isotopic composition of the meltwater with time as the column was melted. The entire column took 68 hours to melt. We then conducted a second experiment to examine whether there was any significant isotopic redistribution along the snow column before meltwater flowed from the base. The initial conditions were identical to those in the first experiment, but we shut off the heat lamp as soon as water began to flow from the base of the column (this took 13 hours, and the snow column height was reduced from 38 to 32 cm). The column was immediately turned on its side and placed in a −15°C cold room to freeze. When frozen, the snow column was removed from its Plexiglas casing and sectioned into 1-cm-thick pieces along its length.

2.4. Analytical Methods

Each water sample collected during the field experiment was split into two parts, one for determining isotope ratios and the other for measuring REE concentrations. The aliquots to be analyzed for REE concentrations were acidified with ultrapure

Table 1. Rare Earth Element Tracers Applied During This Study

Tracer	Date Applied	Height, cm	Concentration Applied		Volume Applied		Baseline	
			Pan, ppm	Pit, ppm	Pan, mL	Pit, mL	New Snow,[a] ppt ± 1σ	Control Pit,[b] ppt ± 1σ
Dy	Feb. 18, 1998	339	26.5	28.4	3043	2915	2 ± 7	0 ± 1
Tb	Feb. 12, 1998	316	24.1	24.7	2979	2978	0 ± 1	0 ± 0
Gd	Feb. 5, 1998	255	22.2	23.7	2985	2979	0 ± 1	0 ± 0
Eu	Feb. 2, 1998	228	26.3	21.8	3077	3024	1 ± 2	16 ± 24
Sm	Jan. 21, 1998	203	36.5	34.8	2969	3000	1 ± 1	0 ± 0
Nd	Jan. 16, 1998	186	24.8	24.7	2961	2998	7 ± 8	2 ± 3
Pr	Jan. 6, 1998	140	41.2	46.8	2978	3030	2 ± 3	0 ± 1
Ce	Dec. 11, 1997	102	20.9	22.6	2959	3027	16 ± 15	4 ± 6
La	all dates	all	24.4 ± 2.6	24.6 ± 4.5			8 ± 13	16 ± 28

[a]Number of analyses is 26.
[b]Number of analyses is 12.

nitric acid (SeaStar®) to make a 1 wt% HNO_3 solution. The REE concentrations were measured using a high-resolution inductively coupled plasma-mass spectrometer (ICP-MS) (Finnigan Element) at Dartmouth College. The analytical accuracy was better than 5% for all samples.

The field and laboratory samples were analyzed for $\delta^{18}O$ using the method of CO_2 equilibration [*IAEA*, 1981]. The $^{18}O/^{16}O$ ratio was determined using an isotope ratio mass spectrometer, and results were expressed in the δ notation as the parts per thousand difference relative to Vienna standard mean ocean water (VSMOW). The precision of the $\delta^{18}O$ measurements was 0.1‰ (1σ).

3. Results

3.1. REEs as Markers of Snow Layers

The concentration and the amounts of each solution sprayed on the snow are listed in Table 1. The average REE concentrations of new snow and the samples from the control pit are also included in Table 1. The spike solutions are at least 6 orders of magnitude greater than the natural REE abundances in snow.

The positions of the REE tracers in the three snow pits are shown in Figure 1. Except for Tb, the concentration peaks for each REE element are within the same 10 to 20 cm height interval in all three snow profiles. This indicates that differential settling of snow and snow drifting were not significant. All tracers, except Ce, were applied after the initial compaction of new snow.

Plots of the concentrations of the REE tracers in pit B as a function of depth in the pack are shown in Figure 2. Most tracers are clearly seen in the profile. For each tracer peak, there is a corresponding La peak. In pits A, B, and C the concentration of La equals the sum of all other tracer concentrations within 7% on average (50% maximum). This suggests that the REEs behaved similarly and did not have a specific elution order. Although the original tracer solutions all have similar concentrations, the concentrations seen in Figure 2 vary by 2 orders of magnitude, from a few parts per billion (ppb) for Nd and Sm (Figure 3) to ~180 ppb for Gd. Some variations may have been caused by the uneven application of the tracers. The tracers are colorless in solution, so they offer no visual clue that could help in spraying them evenly over the snow surface. Perhaps as a result, a few tracers have low concentrations in one or two of the three pits. For example, the concentration of Sm is very low (1 ppb) in pit B, but it is high (95 ppb) in pit A at the 135 cm level. Nd is the only tracer having low concentrations in all pits, and it was the only tracer applied during a significant winter melt event. It was applied on Jan-

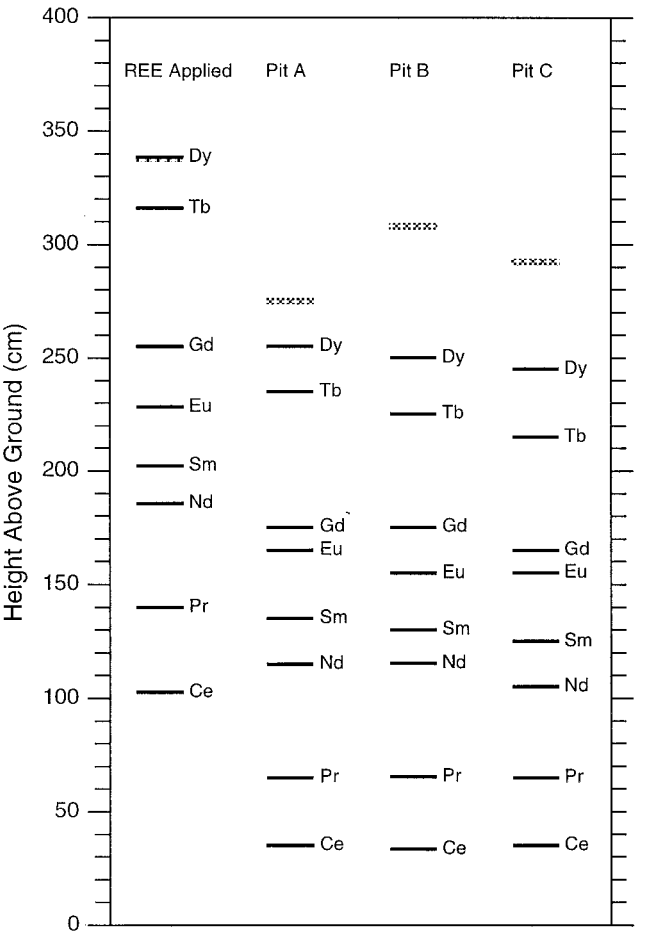

Figure 1. Position of the REE layers in the three snow pits plotted alongside their height in the snowpack on the day they were applied. Pit A was excavated on March 23, 1998, and is 2 m to the north of pits B and C. Pits B and C were 2 m apart on an east-west line and were dug on April 9, 1998. The hatched line indicates the position of the snow surface on the day the pits were excavated.

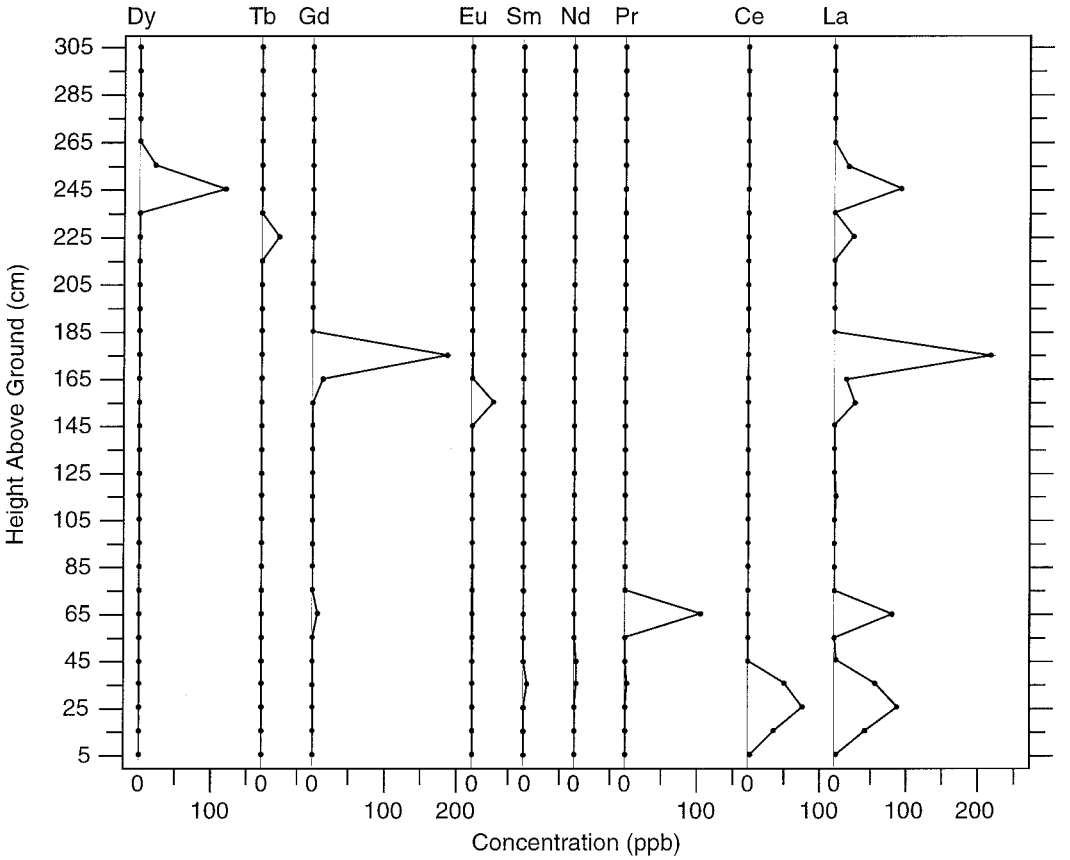

Figure 2. Plots showing concentration of the different REEs in pit B, including the common tracer La, against the height above the base of the snowpack.

uary 16, and the tipping bucket measured ~600 L (~8 cm of snow) of melt on January 15 and 16. It also rained on January 16 and 17, after the Nd had been applied. The infiltrating snowmelt and rainwater mobilized the Nd and flushed most of it from the pack [*Feng et al.*, 2001]. Despite its low concentration, however, the original position of Nd is still visible in all pits at about the 115-cm level (Figures 1 and 3). In pit B the concentration of both Nd and Sm is elevated (6 ppb) at a layer 35–45 cm above the ground (Figure 3). This layer corresponds to an ice layer that is probably responsible for retaining some of the tracers.

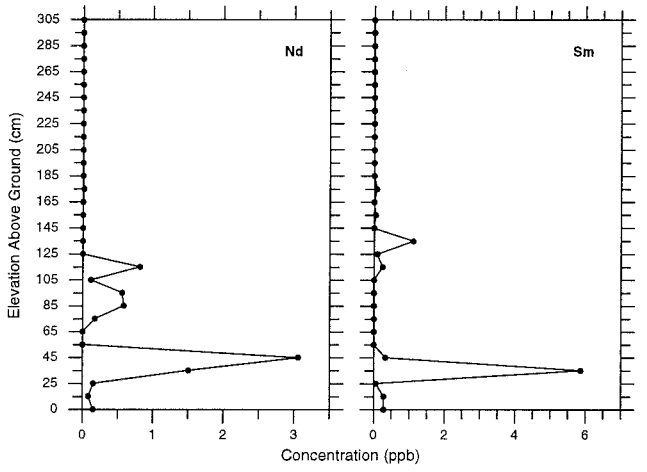

Figure 3. Concentration of Nd and Sm in pit B plotted against height above the base of the snowpack.

In summary, the REE tracers served as good markers for the snow layers. In interpreting our data we will assume that the snowpack did not compact further after the snow pits were sampled. This is a reasonable assumption, given that the snow pits sampled 2 weeks apart show the REE tracers at similar heights, and that most of the compaction has been found to occur shortly after snowfall [*Colbeck*, 1978]. We also assume that all the meltwater was generated at the snow surface so that the source of the daily snowmelt can be obtained by measuring the height of the snowpack. Early in the season, some melt may be generated by ground heat; during the main melt, however, the bulk of the tracers appear in meltwater in the reverse order in which they were applied. This indicates that the pack melted from the top down [*Taylor et al.*, 1998].

3.2. Isotopic Composition of New Snow, Snowpack, and Meltwater Samples

The isotopic data are summarized in Figures 4–7. Figure 4 plots 24 new snow samples, 31 snow pit samples, and 16 meltwater samples. This diagram is constructed in the following way: (1) The $\delta^{18}O$ of each new snow sample was scaled, using its original snow depth and its density, to show which snowfalls contributed to intervals in pit B delineated by the REE markers. For example, three new snow samples were collected between the dates when Pr and Nd were applied. These three samples are plotted between the height of Pr and Nd in pit B. (2) The $\delta^{18}O$ of each sample from pit B was plotted versus its

height above ground. The dashed horizontal lines indicate the positions of the REE tracers in the pit. (3) The $\delta^{18}O$ value of the meltwater is plotted against the height of the snowpack on the day when the water was collected, reflecting our assumption that meltwater originated at the top of the pack. We plotted only morning meltwater collected after the snow pit B was sampled.

Four important observations are illustrated in Figures 4–7. First, there is some correspondence between the isotopic composition of the new snow and its composition in the snowpack, but the correspondence is not strong, indicating that isotopic redistribution has occurred. Second, the variability of isotopic composition decreases from the new snow to the snow pit and to the snowmelt. This is clearly illustrated in Figure 5, which shows frequency distributions of isotopic values for all three types of samples. Despite the homogenization within the snowpack before the onset of the melt season, the mean isotopic composition did not change significantly relative to our experimental precision. The $\delta^{18}O$ of the new snow ranged from -9.2 to $-22.8‰$, with a weighted mean (based on the depth of the snowfall and its density) of $-14.3‰$, and the snow pit samples ranged from -10.9 to $-18.3‰$, with a mean of $-14.1‰$. The meltwater samples ranged from -13.2 to $-17.3‰$. It is difficult to calculate the weighted mean for the snowmelt owing to insufficient sampling frequency. Third, regardless of the isotopic composition of individual layers in the snowpack, the meltwater becomes isotopically heavier as more of the pack is melted. This is shown in Figure 6a, in which the $\delta^{18}O$ values of all of the meltwater samples are plotted against the fraction of the melted water to the total meltwater measured by the melt pan (F). The initial melt was similar to the average $\delta^{18}O$ value of the pack but decreased by $3‰$ when $F \approx 0.1$. After this point the isotopic composition of the melt became progressively heavier, following an exponential trend until the pack was completely melted. The first ~50% of the meltwater was isotopically lighter than the average of the snow pit samples ($-14.1‰$). Finally, on a given day the $\delta^{18}O$ values of meltwater are systematically lower at low flow rates than at high flow rates. Figure 7 shows two examples for the snow layers between the Ce and Pr and the Sm and Eu markers. The $\delta^{18}O$ values of meltwater collected on the same day are lower in the morning (low flow rate) than in the afternoon.

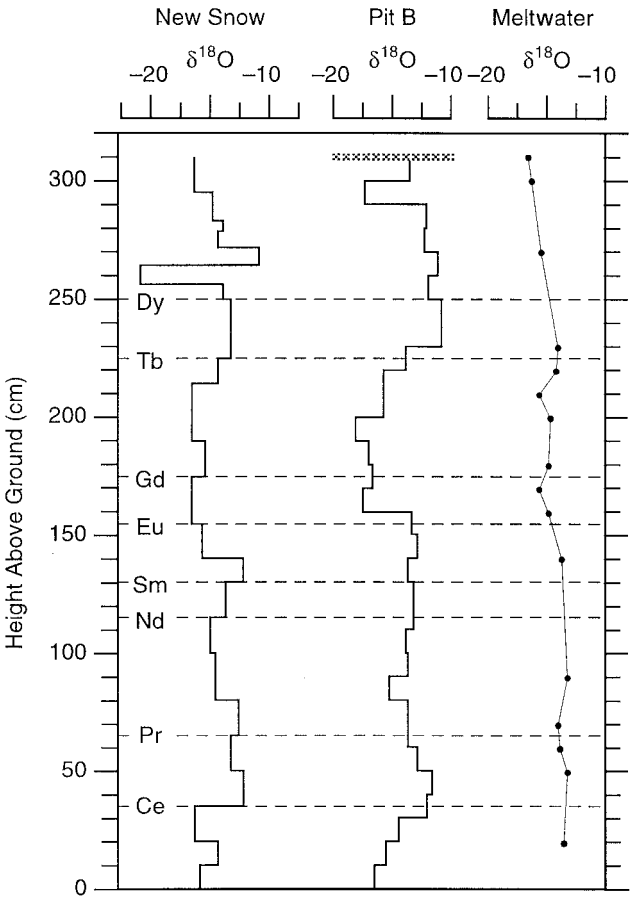

Figure 4. Values of $\delta^{18}O$ for new snow, pit B, and meltwater samples versus the height in the snowpack (see the text). The new snows were collected between November 26 and April 16. The hatched line in the pit B column indicates the position of the snow surface on April 9 when the pit was sampled. The last meltwater sample was collected June 23, and only morning meltwater samples collected after April 9 are plotted.

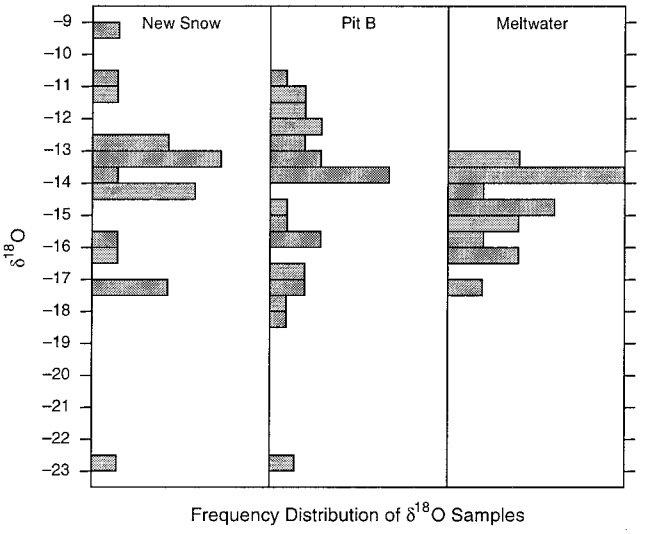

Figure 5. Histograms showing the $\delta^{18}O$ variation in the new snow, pit B, and meltwater samples.

3.3. Results of Cold Room Experiments

The isotopic composition of the meltwater from our first cold room experiment is shown in Figure 6b. There are many similarities between this result and the field observation shown in Figure 6a. As in Figure 6a, the $\delta^{18}O$ of the meltwater decreased as F increased from 0 to 0.05. This decrease was then followed by an exponential increase, reaching the mean $\delta^{18}O$ value of the pack at $F = 0.35$. The maximum isotopic depletion in ^{18}O of the meltwater from the original snow column was $\sim 2‰$.

Figure 8 shows the isotopic composition of the snow (solid circles) in the second cold room experiment, which was designed to test for isotopic redistribution before meltwater started to flow from the base. The snow at the top is isotopically heavier than the original snow, and the snow in the lower section is slightly depleted in ^{18}O.

4. Discussion

4.1. Isotopic Redistribution in the Snowpack

We found that the snowpack was isotopically less variable than the new snow, reflecting isotopic redistribution within the

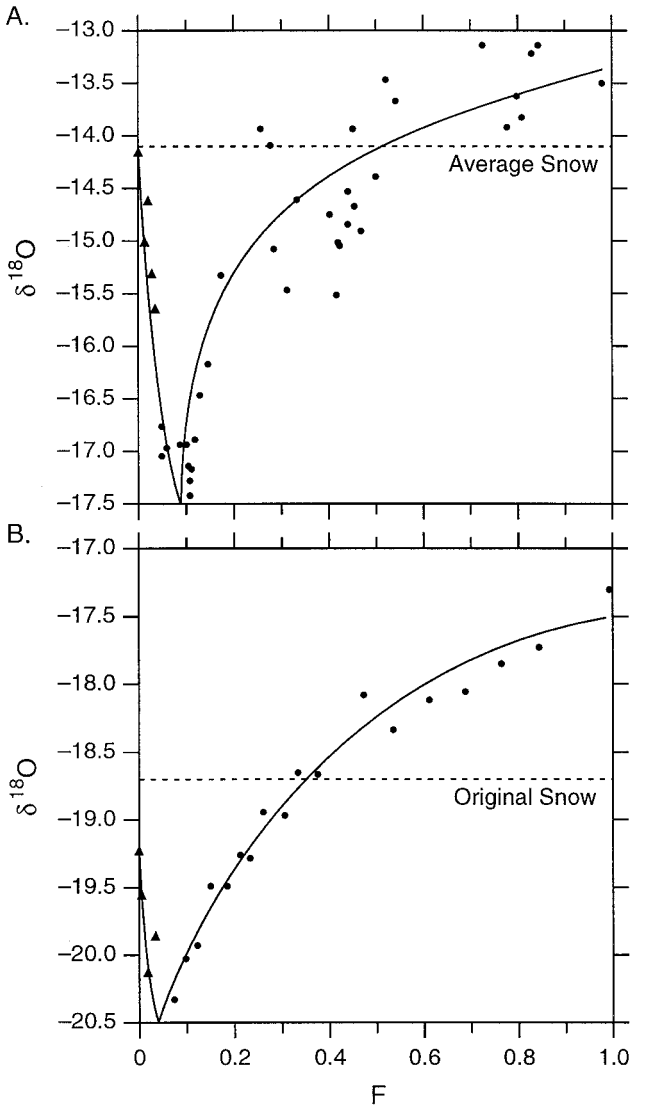

Figure 6. The $\delta^{18}O$ values of meltwater samples plotted against F, the cumulative melt volume divided by the total melt volume: (a) 42 meltpan samples from CSSL and (b) 22 samples from the laboratory column experiment. The curves in the figures are drawn to guide the observation. The triangular data points are early meltwaters that show the opposite trend of isotopic composition variation from the remaining samples.

snowpack. Others [*Árnason et al.*, 1973; *Judy et al.*, 1970] have reported similar results. A number of processes during snow metamorphism may cause isotopic redistribution in a snowpack. These processes all involve phase changes of water among solid, liquid, and vapor. Vapor transport occurs shortly after new snow is deposited and results in large snow crystals growing at the expense of small ones [*Colbeck*, 1978]. If an entire grain is sublimated and recrystallized locally, there is no isotopic redistribution. However, if the vapor moves a significant distance before it is deposited, water from one layer can be transported to another layer. In addition, partial condensation may occur during the vapor transport, which causes isotopic depletion in ^{18}O of the vapor phase and additional isotopic redistribution. Vapor transport has been reported in subarctic packs where large temperature gradients drive vapor from warm to cold areas, usually from the bottom to the top of the pack [*Sturm and Benson*, 1997; *Friedman et al.*, 1991; *Sommerfeld et al.*, 1991].

Melt flow is probably the dominant process causing isotopic redistribution in temperate snowpacks, such as those at CSSL. On a warm day the snow at the surface may melt, and the melt transports water from the surface to layers below, where it may refreeze. As in the case of vapor condensation, freezing is also associated with isotopic fractionation, with the water phase being depleted in ^{18}O. Again, freezing of water as it percolates down the snow column results in isotopic redistribution in addition to simple mass transfer.

In the phase transitions described above, vapor may be lost from the top of the pack, and water may be drained from the bottom. Both processes may cause the snowpack to become enriched in ^{18}O compared to its original composition [*Stichler*, 1987]. In our field experiment the mean isotopic composition of the snow did not change significantly, relative to our experimental precision, before the melt season began, suggesting that the mass loss through vapor and melt was limited. However, isotopic redistribution within the pack is evident.

4.2. Isotopic Evolution of Snowmelt

If melting largely occurred at the surface, and if there were no interaction between the water and the ice as water percolated down the snow column, we would expect the meltwater to inherit the isotopic composition of the snow layer being melted. What we observed, however, was a systematic increase of $\delta^{18}O$ in the meltwater, as the melt season or the melt experiment progressed, irrespective of the composition of the source snow. Laboratory data presented by *Herrmann et al.*

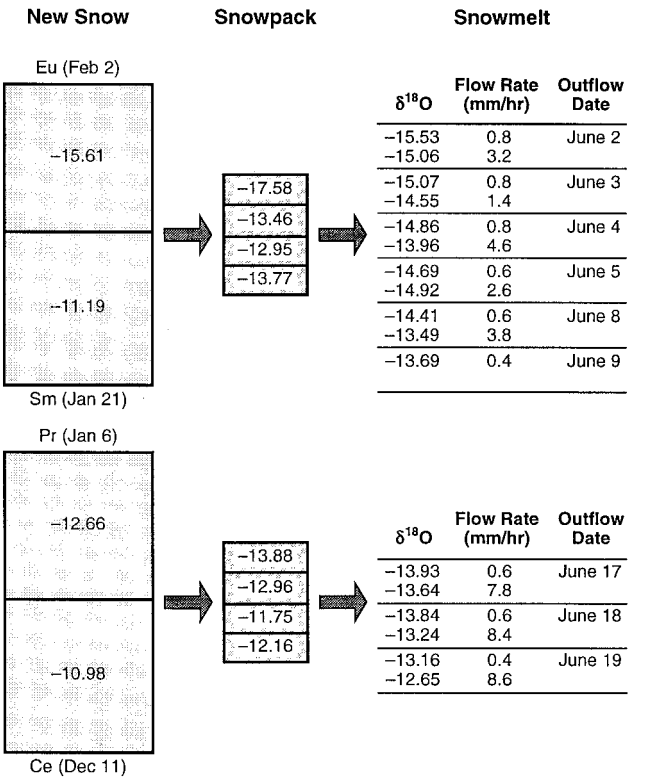

Figure 7. Comparison of the $\delta^{18}O$ values of new snows with their resulting snowpack layers and the melt generated from these layers. Note that the $\delta^{18}O$ values of meltwater are systematically lower at low flow rates than at high flow rates.

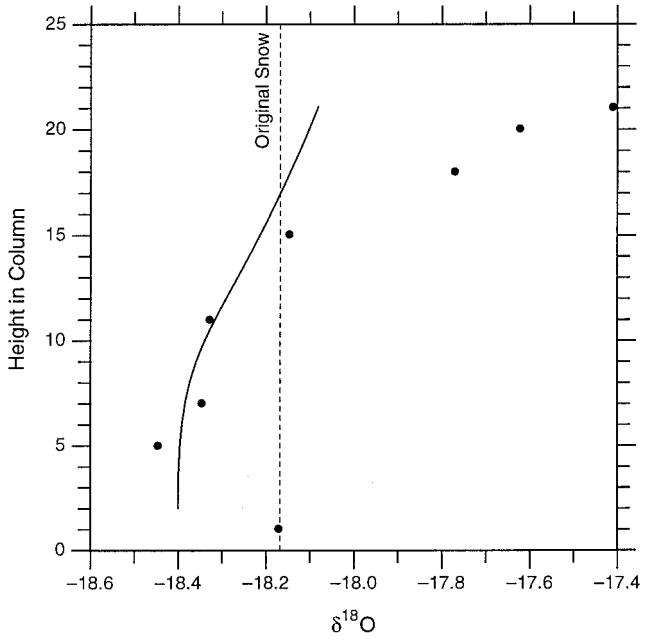

Figure 8. The $\delta^{18}O$ values of 1-cm ice segments versus height in laboratory snow column. The experiment was designed to examine isotopic redistribution before meltwater appeared at the base. The curve is the isotopic composition of the snow column predicted by our model. Note the upper 25% of the column is more enriched in ^{18}O than predicted by the model, indicating isotopic fractionation enrichment by evaporation.

[1981] show that both the meltwater and the remaining snow in their snow columns became increasingly enriched in ^{18}O as melt progressed. Many other field studies have shown that the mean $\delta^{18}O$ of a snowpack increases over the winter [*Dinçer et al*., 1970; *Árnason et al*., 1973; *Martinec et al*., 1977; *Rodhe*, 1981; *Mast et al*., 1995; *Shanley et al*., 1995]. These observations reflect the fact that isotopically light water is lost early in the season, causing the snowpack and the meltwater to become progressively heavier [*Árnason et al*., 1973; *Rodhe*, 1998].

The lack of correspondence between the $\delta^{18}O$ of snow and that of meltwater suggests that isotopic exchange occurs between ice and percolating water. When snow melts at the surface, little isotopic fractionation occurs because the entire layer is melted. As this meltwater percolates down the snowpack, however, isotopic exchange takes place between the water and the ice. During this exchange, liquid water would become relatively depleted in ^{18}O relative to ice, because at equilibrium the $\delta^{18}O$ of the water is 3.1‰ lower than that of the ice [*O'Neil*, 1968]. Two factors would affect the extent of isotopic exchange: the effective rate of exchange and the surface area available for the exchange. We use the effective rate of exchange to describe the overall effects of the rate constant of the exchange, the depth of the snowpack, and the flow velocity. The rate constant characterizes the intrinsic nature of the exchange kinetics, and the depth and the flow velocity determine the contact time between water and ice.

The surface area available for the water-ice exchange is difficult to characterize. Although the grain size distribution is an obvious variable, this distribution changes throughout the season. Snow metamorphism causes the snow crystals to become progressively larger, with most changes occurring within the first few days after precipitation [*Colbeck*, 1978]. The flow mechanism, e.g., homogenous flow verse finger flow, also affects the effective surface area. In finger flow, meltwater is in contact with only a small area of the pack, and the actual flow velocity is greater than that of homogenous flow given the same melt rate. To quantify the concepts described above, we developed a 1-D model for the isotopic evolution of snowmelt. We tested the model using our snow column and field data.

4.3. A Physically Based 1-D Model for Isotopic Evolution of Snowmelt

Búason [1972] presented the only model describing the isotopic variability of snowmelt. His model considers the rate of water percolation and kinetics of ice-water exchange, but the isotopic exchange occurs between water and the bulk ice rather than only at the ice surface. Our model considers the effective surface area by letting only a fraction of the ice participate in the isotope exchange. To keep our model simple, we assume constant melt rate, homogenous flow, and constant surface area during the melting process.

With a constant flow velocity, the governing equation for the liquid phase is

$$\frac{\partial R_{\text{liq}}}{\partial t^*} + u^* \frac{\partial R_{\text{liq}}}{\partial z^*} = \frac{\partial}{\partial z^*}\left[D^* \frac{\partial R_{\text{liq}}}{\partial z^*}\right] + k_r\gamma(R_{\text{ice}} - \alpha R_{\text{liq}}), \tag{1}$$

where R_{liq} and R_{ice} are the $^{18}O/^{16}O$ ratio in the water and ice, respectively, u^* is the percolation velocity, D^* is the dispersion coefficient, t^* is the time, z^* is the depth from the surface, k_r is the isotope exchange rate constant, and α is the equilibrium fractionation factor between ice and water at 0°C. We use the parameter γ to quantify the fraction of ice participating in the isotopic exchange,

$$\gamma = \frac{bf}{a + bf}, \tag{2}$$

with f denoting the fraction of ice that is involved in isotopic exchange and a and b denoting the mass of oxygen in water and in ice, respectively, per unit depth of snow. This parameter is related to the surface area. The isotopic composition of ice changes only through its interaction with the water, and so the governing equation is

$$\frac{\partial R_{\text{ice}}}{\partial t^*} = k_r(1 - \gamma)(\alpha R_{\text{liq}} - R_{\text{ice}}). \tag{3}$$

To further simplify the model, we assume that dispersion is not significant and therefore that $D^* = 0$.

For discussion and comparison purposes it is convenient to nondimensionalize the governing equation. We define nondimensional time, t, and depth, z, as

$$z = \frac{z^*}{Z} \qquad t = \frac{t^* u^*}{Z}, \tag{4}$$

where Z is the total depth of the snow column before melting starts. The nondimensional governing equation then becomes

$$\frac{\partial R_{\text{liq}}}{\partial t} + \frac{\partial R_{\text{liq}}}{\partial z} = \psi\gamma(R_{\text{ice}} - \alpha R_{\text{liq}}) \tag{5}$$

for water and

$$\frac{\partial R_{\text{ice}}}{\partial t} = \psi(1 - \gamma)(\alpha R_{\text{liq}} - R_{\text{ice}}) \tag{6}$$

for ice, where

$$\psi = \frac{k_r Z}{u^*}. \tag{7}$$

The nondimensional equations combine three constants, k_r, Z, and u^*, into one dimensionless constant ψ, which quantifies the effectiveness of isotopic exchange. If we keep k_r constant, we can increase isotopic exchange by either increasing snow depth or decreasing the flow velocity because both parameters affect the time of contact between water and ice.

The parameter ψ accounts for the observed daily variations in the $\delta^{18}O$ of the snowmelt (Figure 7). On a given day the depth of the pack can be considered constant, but the melt rate may differ by an order of magnitude. A high flow rate reduces the contact time between water and ice and thus limits the degree of isotopic depletion in ^{18}O of the meltwater. As a result, the $\delta^{18}O$ values of afternoon samples are consistently higher than those of morning samples.

4.4. Modeling the Cold Room Experiment

We used the model described in section 4.3 to fit the isotopic composition of the melt from the snow column experiment. To describe the water flow, we used a reduced form of Richards' equation that has been applied by a number of authors, including *Colbeck* [1972] and *Hibberd* [1984],

$$\phi(1 - S_i)\frac{\partial S}{\partial t^*} + \frac{K\partial S^n}{\partial z^*} = 0, \tag{8}$$

where S is effective water saturation, which relates to the total water saturation S_w and irreducible water saturation S_i (water held in place by capillary forces) as

$$S = \frac{S_w - S_i}{1 - S_i}. \tag{9}$$

The parameter n is an empirical exponent and ϕ is porosity of snow. K is hydraulic conductivity and is given by

$$K = \frac{\rho k g}{\mu}, \tag{10}$$

where k is the intrinsic permeability and ρ, g, μ are the water density, gravitational acceleration, and water viscosity, respectively.

The percolation velocity u^* is

$$u^* = \frac{K}{\phi(1 - S_i)}\frac{S^n}{(S + \beta)} \tag{11}$$

[*Hibberd*, 1984], where $\beta = S_i/(1 - S_i)$. We assume that initially the snow column is at the irreducible saturation level, and that at $t^* = 0$ the effective water content at the surface is brought up from zero to a certain value and is kept at this value for the entire experiment. The velocity of the saturation wave front V^* is

$$V^* = \frac{KS^{n-1}}{\phi(1 - S_i)} \tag{12}$$

[*Hibberd*, 1984], and the corresponding nondimensional water and wave velocities are

Table 2. Model Parameters Used in This Study

Parameter	Snow Column	CSSL Field Data
Bulk density, g cm^{-3}	0.53	0.42
Melt rate, cm h^{-1}	0.5	0.15
Porosity	0.44	0.57
Irreducible water content, S_i	0.04	0.04
Saturated water content, S	0.049	0.0243
Intrinsic permeability, m^2	1.2×10^{-9}	2.3×10^{-9}
Initial $\delta^{18}O$, ‰	−18.7	−14.1
Percent of ice exchanging	30%	37%
α	1.0031	1.0031
γ	0.8	0.8
ψ	0.9	0.9

$$u = \frac{\phi(1 - S_i)u^*}{K} \tag{13}$$

and

$$V = \frac{\phi(1 - S_i)V^*}{K}. \tag{14}$$

We have a moving boundary condition at the surface defined by the melt rate of the experiment. The isotopic ratio of the water at the upper boundary is the bulk isotopic ratio of the snow at the surface. This value is the weighted average of the three water components: the liquid, the outer part of the ice crystals participating in the exchange reaction, and the interior part of the ice crystals. The lower boundary is set at the wave front before the percolating water reaches the bottom of the column and at the bottom afterward.

Snow parameters that need to be input to the model include the intrinsic permeability, bulk density, melt rate, irreducible water content (S_i), and the value of the exponent n. From these the hydraulic conductivity, porosity, and the effective saturation of the snow are calculated. In the case of our laboratory experiment we used an intrinsic permeability of 1.2×10^{-9} m^2, obtained using *Shimizu*'s [1970] relationship between intrinsic permeability, bulk density, and grain size. This value is consistent with that measured for snow having a comparable porosity (1.4×10^{-9} m^2 [*Wankiewicz*, 1979]). The bulk density and the melt rate were measured in our experiment. We used 4% for S_i [*Jordan*, 1991] and 3% for n [*Colbeck and Anderson*, 1982; *Wankiewicz*, 1979]. The nondimensional parameters ψ and γ are obtained by fitting the model to the isotope data of the melt. Table 2 lists the values used for the different parameters in each of the model runs.

Figure 9b shows the model results for the laboratory experiment plotted as $\delta^{18}O$ of the melt versus the fraction of snow melted. There are two curves in Figure 9b. The dashed curve is generated from the model using the parameters listed in Table 2. We optimized the parameters to best fit the overall curvature of the observation rather than using the usual least squares technique. Choosing other values of ψ or γ does not fit the earlier or the later segment of the observations. The solid curve is calculated by increasing the initial isotopic composition of the snow in the column by 0.3‰. This parameterization nicely reproduces the exponential trend of the isotopic evolution and gives 0.01 hour^{-1} for the rate constant of isotopic exchange and 30% for the fraction of ice participating in the exchange process.

The 0.3‰ offset may have been caused by evaporation from

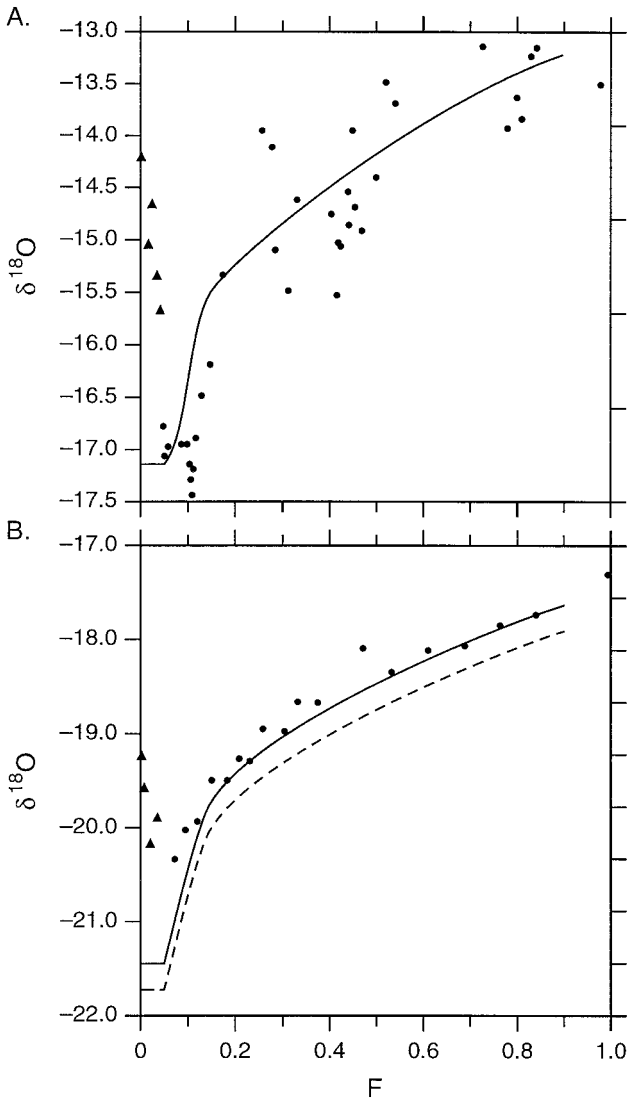

Figure 9. Modeled (curves) versus the measured isotopic compositions of meltwater: (a) all CSSL melt pan samples and (b) cold room snow column samples. The dashed curve in Figure 9b is the best fit to the overall shape (curvature) of the data, and the solid curve is calculated using the same parameters but assuming 0.3‰ enrichment in ^{18}O of ice at the snow surface. The triangular data points in Figure 9b are waters thought to be a mixture of melted basal snow and isotopically light water.

the snow surface, a process not incorporated into the model but documented by *Herrmann et al.* [1981]. An isotopic enrichment in ^{18}O at the snow surface was observed in our second column experiment (Figure 8). The top 4 cm of snow show an average increase of 0.6‰ in $\delta^{18}O$ over the original snow. The curve in Figure 8 is the predicted isotopic composition of the snow column at the time when the water started to flow from the base. The model matches the isotopic composition of the snow in the middle and lower segment of the column but predicts lower $\delta^{18}O$ values near the top.

The model does not explain the first 5% of the melt (F = 0–0.05). It produces a flat segment, which represents the water that was originally in the pack as irreducible water, and we assumed that this water was in isotopic equilibrium with the bulk snow. After $F = 0.05$ there is an abrupt increase in the $\delta^{18}O$ of the melt. This occurs because we removed the dispersion term, which acts to smooth the curve. However, even if dispersion were considered, the model would not reproduce the decreasing trends in $\delta^{18}O$ for $F < 0.05$ seen in the laboratory and field data. A possible explanation for this early decrease is as follows: in our cold room experiment it took ~13 hours for the column to start draining water at the bottom. During this time, warm air from the heated outflow tube may have melted a small amount of snow at the base. This water would have an isotopic composition similar to the bulk snow, and it did not flow out because of capillary tension. When the wetting front arrived at the bottom, this water mixed with the isotopically depleted water. The contribution of this isotopically heavy water at the base decreased as more water flowed through and eventually became insignificant. A similar process might have occurred in the melt pan at CCSL. However, judging from the isotopic composition at the bottom of the pack (approximately −16‰), it is unlikely in this case. When those samples were collected in December and January, the snowpack was shallow and growing. The melt could have been generated from layers having relatively high $^{18}O/^{16}O$ ratios (e.g., layers between Ce and Pr).

We also applied the model to our field data, and the results are shown in Figure 9a. Here we used measured bulk density, the average daily melt rate, and an intrinsic permeability of 2.3×10^{-9} m^2, a value measured at CSSL for snow having a comparable density [*Colbeck and Anderson*, 1982]. We again used 4% for S_i and 3% for n. We found that we can fit the data well using the same values for ψ and γ as those used in our column experiment. We expected that the ψ value would be much higher because the snow depth is greater than that in the column experiment by a factor of 10, and the average melt rate is lower by a factor of 3. If the rate constant is the same in both cases, the value of ψ should increase by a factor of 30. However, we cannot fit the field data with such a high ψ value. The reason for this is not clear, but a number of assumptions in our model may not be valid for the field conditions. The model assumes that melt rate and surface area are both constant, but we know the melt rate varied significantly at CSSL throughout the season. More controlled experiments will investigate the effects of melt rate and snow grain size on the isotopic composition of the melt.

4.5. Implications of Our Findings

Our observations, and those of others, show that the isotopic composition of a snow core is not necessarily the same as the isotopic composition of the resulting snowmelt. If hydrograph separation is to be conducted throughout spring runoff, the progressive isotopic enrichment in the meltwater needs to be considered. Our model is a first step toward predicting the isotopic trend of the meltwater given the isotopic compositions and depth of the snowpack and the melt rate. There exist general models, such as SNTHERM [*Jordan*, 1991], that calculate snow accumulation, compaction, and mass transport using meteorological parameters. By attaching the isotopic model to a general snow model, one could predict the isotopic evolution of snowmelt at a meteorologically instrumented location.

The isotopic evolution of snowpacks and snowmelt may be linked with their chemical evolution, making it possible to study processes affecting solute elution during melting. The isotopic and chemical compositions of meltwater can be

broadly interpreted as representing three fundamental groups of processes: (1) those controlling the metamorphism and melting of individual snow layers, (2) those controlling the transport pathways by which meltwater percolates through the snowpack, and (3) those controlling the interaction of the meltwater with the ice grains during transport. Although all three sets of processes affect both the isotopic and chemical compositions of snowpacks and snowmelt, the relative sensitivities may vary significantly. For example, the chemical concentration of solutes in snowmelt have been found to be positively related to flow rate in some experiments but negatively in others [*Feng et al*., 2001], while the $\delta^{18}O$ should always be positively related to the flow rate. Differences between the behavior of isotopes and solutes can elucidate snowpack processes and contribute to the understanding of the timing and magnitude of the ionic pulse, which has important consequences for surface water ecosystems [*Johannessen and Henriksen*, 1978; *Colbeck*, 1981; *Bales et al*., 1989].

Finally, there is great interest in using alpine ice cores for paleoclimate studies [*Thompson et al*., 1998]. These studies require that the $\delta^{18}O$ of precipitation track surface temperature, that the $\delta^{18}O$ is preserved sequentially in a snow or ice profile, and that isotopic modification by vapor and water movement is insignificant. Only a few researchers have studied how glacier snow and firn are changed isotopically by water or vapor flow [e.g., *Johnsen*, 1977; *Stichler*, 1987]. The process by which snow becomes firn smoothes $\delta^{18}O$ variations in the record of $\delta^{18}O$ versus depth [*Johnsen*, 1977]. Visible melt layers in the Greenland ice cores indicate the presence of water. Our work may help in determining the magnitude of the possible consequences of these processes and in assessing the accuracy of $\delta^{18}O$ in ice cores as a proxy for temperature.

5. Conclusions

We found the REE tracers to be effective markers for the snowpack, and we used them to determine the position of snow layers. We saw a weak correlation between the isotopic composition of the new snow and the snowpack and no correlation between the snow and the snowmelt. At CSSL, snow metamorphism causes isotopic homogenization of the snowpack. The isotopic composition of the snowmelt became progressively heavier as the pack melted in both the field and cold room experiments. Additionally, our field data showed a relationship between flow rate and the isotopic composition of the melt; for a given day the morning samples were isotopically lighter and have lower flow rates than the afternoon samples. These variations indicate that isotopic exchange occurred between the liquid and ice as water flowed through the snowpack, resulting in depletion of ^{18}O in the liquid phase.

We developed a 1-D model that calculates the isotopic compositions of the meltwater at a constant melt rate and surface area for water-ice isotopic exchange. Fitting the model to our laboratory data, we obtained 0.01 hour^{-1} for the exchange rate constant (k_r) and 0.30 for the fraction of ice (f) that participated in the isotopic exchange with water. However, we were not able to fit the field data using the same value of k_r. Instead, the best fit yielded 4×10^{-4} hour^{-1} for this parameter. Because a number of the assumptions made for the model are invalid in the field experiment, the estimate of k_r may not be correct. More controlled experiments are needed to adequately parameterize the model.

The isotopic homogenization of snowpacks, progressive ^{18}O enrichment of snowmelt, and dependence of snowmelt ^{18}O on melt rate are potentially important for studying snowmelt hydrology using stable isotopes, understanding the mechanisms that cause ionic pulses in snowmelt, and using ^{18}O in ice cores for paleoclimate investigations.

Acknowledgments. Support for this work comes from the Department of the Army (AT-24 Snow) and NSF grants EAR-9357931, ATM-9628759, EAR-9814121, and EAR-9903281. The Central Sierra Snow Laboratory is owned by the U.S. Forest Service and operated by the University of California, Berkeley. We thank the refrigeration crew at CRREL and M. Hren for technical assistance.

References

Árnason, B., T. Búason, J. Martinec, and P. Theodorsson, Movement of water through snowpack traced by deuterium and tritium, in *The Role of Snow and Ice in Hydrology*, *Proceedings of the Banff Symposia*, *September 1972*, *IAHS Publ*., *107*, 299–312, 1973.

Bales, R. C., R. E. Davis, and D. A. Stanley, Ion elution through shallow homogeneous snow, *Water Resour. Res*., *25*, 1869–1877, 1989.

Bottomley, D. J., D. Craig, and L. M. Johnston, Oxygen-18 studies of snowmelt runoff in a small preCambrian shield watershed: Implications for streamwater acidification in acid-sensitive terrain, *J. Hydrol*., *88*, 213–234, 1986.

Búason, T., Equation of isotope fractionation between ice and water in a melting snow column with continuous rain and percolation, *J. Glaciol*., *11*, 387–405, 1972.

Buttle, J. M., Isotope hydrograph separations and rapid delivery of pre-event water from drainage basins, *Prog. Phys. Geogr*., *18*, 16–41, 1994.

Colbeck, S. C., A theory of water percolation in snow, *J. Glaciol*., *11*, 369–385, 1972.

Colbeck, S. C., The physical aspects of water flow through snow, *Adv. Hydrosci*., *11*, 165–206, 1978.

Colbeck, S. C., A simulation of the enrichment of atmospheric pollutants in snow cover runoff, *Water Resour. Res*., *17*, 1383–1388, 1981.

Colbeck, S. C., and E. A. Anderson, The permeability of a melting snow cover, *Water Resour. Res*., *18*, 904–908, 1982.

Dinçer, T., B. R. Payne, T. Florkowski, J. Martinec, and E. Tongiorgi, Snowmelt runoff from measurements of tritium and oxygen-18, *Water Resour. Res*., *6*, 110–124, 1970.

Feng, X., C. E. Renshaw, and S. Taylor, Impact of uncertainty in the isotopic composition of snowmelt on hydrograph separation of spring runoff, *Eos Trans. AGU*, *79*(45), Fall Meet. Suppl., F269, 1998.

Feng, X., J. W. Kirchner, C. E. Renshaw, R. Osterhuber, B. Klaue, and S. Taylor, A study of solute transport mechanisms using rare earth element tracers and artificial rainstorms on snow, *Water Resour. Res*., in press, 2001.

Friedman, I., C. Benson, and J. Gleason, Isotopic changes during snow metamorphism, in *Stable Isotope Geochemistry: A Tribute to Samuel Epstein*, vol. 3, edited by H. P. Taylor Jr., J. R. O'Neil, and I. R. Kaplan, pp. 211–221, Geochem. Soc., St. Louis, Mo., 1991.

Genereux, D., Quantifying uncertainty in tracer-based hydrograph separations, *Water Resour. Res*., *34*, 915–919, 1998.

Herrmann, A., M. Lehrer, and W. Stichler, Isotope input into runoff systems from melting snow covers, *Nord. Hydrol*., *12*, 309–318, 1981.

Hibberd, S., A model for pollutant concentrations during snow-melt, *J. Glaciol*., *30*, 58–65, 1984.

Hooper, R. P., and C. A. Shoemaker, A comparison of chemical and isotopic hydrograph separation, *Water Resour. Res*., *22*, 1444–1454, 1986.

International Atomic Energy Agency (IAEA), Stable isotope hydrology, *Tech. Rep. Ser. IAEA*, *210*, p. 337, Vienna, Austria, 1981.

Johannessen, M., and A. Henriksen, Chemistry of snow meltwater: Changes in concentration during melting, *Water Resour. Res*., *14*, 615–619, 1978.

Johnsen, S. J., Stable isotope homogenization of polar firn and ice, in *Isotopes and Impurities in Snow and Ice*, *IAHS-AISH Publ*., *118*, 210–219, 1977.

Jordan, R. E., A one-dimensional temperature model for a snow cover,

CRREL Spec. Rep. 91-16, U.S. Army Cold Reg. Res. and Eng. Lab., Hanover, N. H., 1991.

Judy, C., J. R. Meiman, and I. Friedman, Deuterium variations in an annual snowpack, *Water Resour. Res*., *6*, 125–129, 1970.

Martinec, J., H. Moser, M. R. de Quervain, W. Rauert, and W. Stichler, Assessment of processes in the snowpack by parallel deuterium, tritium and oxygen-18 sampling, in *Isotopes and Impurities in Snow and Ice*, *IAHS AISH Publ*., *118*, 220–231, 1977.

Mast, A. M., C. Kendall, D. H. Campbell, D. W. Clow, and J. Black, Determination of hydrologic pathways in an alpine-subalpine basin using isotopic and chemical tracers, Loch Vale Watershed, Colorado, USA, in *Biogeochemistry of Seasonally Snow-Covered Catchments*, *IAHS Publ*., *228*, 263–270, 1995.

O'Neil, J. R., Hydrogen and oxygen isotope fractionation between ice and water, *J. Phys. Chem*., *72*, 3683–3684, 1968.

Osterhuber, R., Climate summary of Donner Summit, California 1870–1999, report, Cent. Sierra Snow Lab., Soda Springs, Calif., 1999.

Prowse, T. D., and F. M. Conly, Effects of climatic variability and flow regulation on ice-jam flooding of a northern delta, *Hydrol. Processes*, *12*, 1589–1610, 1998.

Rodhe, A., Spring flood meltwater of groundwater?, *Nord. Hydrol*., *12*, 21–30, 1981.

Rodhe, A., Snowmelt dominated systems, in *Isotope Tracers in Catchment Hydrology*, edited by C. Kendall and J. J. McDonnell, Elsevier Sci., New York, 1998.

Shanley, J. B., C. Kendall, M. R. Albert, and J. P. Hardy, Chemical and isotopic evolution of a layered eastern U.S. snowpack and its relation to stream-water composition, in *Biogeochemistry of Seasonally Snow-Covered Catchments*, *IAHS Publ*., *228*, 329–338, 1995.

Shimizu, H., Air permeability of deposited snow, *Low Temp. Sci*., *Ser. A*, *22*, 1–32, 1970.

Sklash, M. G., and R. N. Farvolden, The role of groundwater in storm runoff, *J. Hydrol*., *43*, 45–65, 1979.

Sommerfeld, R. A., C. Judy, and F. Irving, Isotopic changes during the formation of depth hoar in experimental snowpacks, in *Stable Isotope Geochemistry: A Tribute to Samuel Epstein*, vol. 3, edited by H. P. Taylor Jr., J. R. O'Neil, and I. R. Kaplan, pp. 205–209, Geochem. Soc., St. Louis, Mo., 1991.

Stichler, W., Snowcover and snowmelt processes studied by means of environmental isotopes, in *Seasonal Snowcovers: Physics, Chemistry, Hydrology*, *NATO ASI Ser*., *Ser. C*, vol. 211, edited by H. G. Jones and W. J. Orville-Thomas, pp. 673–726, Kluwer Acad., Norwell, Mass., 1987.

Sturm, M., and C. S. Benson, Vapor transport, grain growth and depth hoar development in the subarctic snow, *J. Glaciol*., *43*, 42–59, 1997.

Taylor, S., X. Feng, B. Klaue, M. Albert, and J. Kirchner, Using rare earth elements as chemical tracers in snow studies, paper presented at 55th Annual Eastern Snow Conference, Jackson, N. H., 1998.

Thompson, L. G., et al., A 25,000-year tropical climate history from Bolivian ice cores, *Science*, *282*, 1858–1864, 1998.

Wankiewicz, A., A review of water movement in snow, in *Proceedings Modeling of Snow Cover Runoff*, edited by S. C. Colbeck and M. Ray, *CRREL Spec. Rep*., *79-36*, U.S. Army Cold Reg. Res. and Eng. Lab., Hanover, N. H., 1979.

X. Feng and C. E. Renshaw, Department of Earth Sciences, Dartmouth College, Hanover, NH 03755. (xiahong.feng@dartmouth.edu; carl.renshaw@dartmouth.edu)

J. W. Kirchner, Department of Earth and Planetary Science, University of California, Berkeley, CA 94720. (kirchner@seismo.berkeley.edu)

B. Klaue, Department of Geological Sciences, University of Michigan, Ann Arbor, MI 48109. (bklaue@umich.edu)

R. Osterhuber, Central Sierra Snow Laboratory, Soda Springs, CA 95728. (randall@sierra.net)

S. Taylor, U.S. Army Cold Regions Research and Engineering Laboratory, 72 Lyme Road, Hanover, NH 03755-1290. (staylor@crrel.usace.army.mil)

(Received May 23, 2000; revised October 24, 2000;
accepted October 25, 2000.)